

# MRI based Brain Tumor Classification using Modified Convolutional Neural Network Model

G. V. Sivanarayana\*<sup>1</sup>, Dr. K. Naveen Kumar <sup>2</sup>

Submitted: 09/10/2023

Accepted : 29/11/2023

Accepted: 11/12/2023

**Abstract:** In recent decades, the Brain Tumor Classification (BTC) by utilizing Magnetic Resonance Imaging (MRI) is an emerging research topic. The existing detection models are complicated, due to the high similarity between normal and abnormal brain tissues and also it consumes an enormous amount of computational time. The automatic brain tumor detection utilizing MRI images is a challenging task for early clinical assessment and treatment planning. This publication proposes a new automatic model to address BTC problems. This study used MRI brain scans from the 2018–2020 Brain Tumor Segmentation (BRATS) databases. Further, the image denoising is performed utilizing Gaussian blur and contour approximation techniques. Finally, the denoised MRI brain images are given as the input to the Modified Convolutional Neural Network (CNN) for brain lesion segmentation and sub-types of tumor classification. The modified CNN model comprises the ReduceLRonPlateau function for early stopping criteria that decreases system complexity and error loss. The extensive experimental investigation demonstrated that the proposed modified CNN model has obtained 99.87%, 99.80%, and 99.63% of accuracy on the BRATS 2018, 2019, and 2020 databases with classification loss of 0.0198, where the obtained results are superior compared to the existing models.

**Keywords:** Brain tumor, classification, convolution neural network, contour approximations, gaussian blur, magnetic resonance imaging and segmentation

## 1. Introduction

Brain tumors—characterized by aberrant and unregulated brain cell proliferation—have become more common in recent decades [1-2]. Brain tumours are usually primary or secondary. Brain tissue produces primary cancers [3]. The secondary tumors are expanded from other body parts to the brain tissues through the bloodstream [4]. The meningioma and glioma are two lethal tumors which lead to severe disorder and even death, therefore, it is necessary to diagnose at an early stage. The brain tumors are categorized into four grades according to the world health organization [5]. The grades one and two tumors indicate meningioma (low-level tumors), and the grades three and four tumors represent glioma (severe-level tumors) [6]. In the clinical practices, the incidence rates of glioma, pituitary and meningioma tumors are approximately 45%, 15% and 15% [7-8]. It is known that the manual tumor analysis is time consuming, invasive and open- to sampling errors, therefore, the computer aided automatic systems are developed for precise and fast brain tumor diagnosis. The automated system improves the diagnostic capabilities of radiologists and clinicians for correct diagnosis [9-10]. In this article we have identified the lapses in the earlier literature and these well incorporated in the form of challenges. The primary challenges encountered in the existing literature pertain to the issues of classification loss and system complexity. The majority of studies related to MRI imaging prioritize the use of CNN

classifiers, as noted by many reviewers.

Consequently, several ways have been devised to showcase the model's capabilities and its efficacy in detecting brain abnormalities. In this work we have considered the limitations and these limitations are considered as motivations and those are highlighted below. However, there are certain limitations of CNN that should be highlighted:

- (1) The effective identification of the disease necessitates a substantial amount of training data.
- (2) When objects are orientated, the convolutional neural network (CNN) demonstrates a lower level of accuracy in recognition.
- (3) The accurate identification of images in the noise poses a significant difficulty.

Hence, this publication presents a novel M-CNN model to enhance the accuracy of BTC. In order to meet the challenges and proposed considered motivations, the well-planned objectives were considered and are highlighted. The aims that have been accomplished in this manuscript are delineated as follows:

- In the preliminary stage, the MRI brain images are obtained from the BRATS 2018, 2019, and 2020 databases. The obtained raw images undergo noise removal and contour identification utilizing Gaussian blur and contour approximation approach, facilitating the desired procedures.

Contributions that are associated in this article are subjected as follows:

- The brain tumor segmentation and sub-type categorization of brain tumors are accomplished by proposing an M-CNN model following the execution of Region of Interest (RoI) analysis.

<sup>1</sup> Computer Science & Engg., GST, GITAM University, Visakhapatnam – 530045, INDIA

ORCID ID : 0000-0001-5915-3595

<sup>2</sup> Computer Science & Engg., GST, GITAM University, Visakhapatnam – 530045, INDIA

ORCID ID : 0000-0003-1024-1329

\* Corresponding Author Email: sgayyi@gitam.edu

- The M-CNN incorporates the ReduceLRonPlateau function into the dense CNN model as a means of implementing early stopping criteria. This inclusion serves to mitigate system complexity and reduce computing time.
- In this improved methodology, a Gaussian Mixture Model (GMM) is employed to mitigate image blur and enhance the accuracy of approximations. This study employs an optimized feature extraction-based approach to accurately detect the condition.
- The efficiency of the M-CNN model is examined in relation to various performance metrics, including accuracy, specificity, Negative Predictive Value (NPV), sensitivity, Positive Predictive Value (PPV), Dice Similarity Coefficient (DSC), and Jaccard Coefficient (JC).

The research manuscript is organized in the following manner. A limited number of articles pertaining to BTC are examined in Section 2. The theoretical and mathematical elucidation of the suggested modified Convolutional Neural Network (CNN) model is presented in Section 3. The results of the simulation and the findings of the updated CNN model are presented in Sections 4 and 5, respectively.

## 2. Related Works

W. Ayadi, et al, [11] implemented a Deep Convolution Neural Network (DCNN) model for BTC. The implemented DCNN model consists of several layers that aim in classifying MRI brain tumors, and the DCNN model's effectiveness was experimentally tested on three online databases such as Radiopaedia, figshare and repository of molecular brain neoplasia database. The simulation results confirmed that the DCNN model delivered a convincing classification performance related to the comparative models. However, the DCNN model needs higher end graphics processing systems, or-else, it consumes more training time. E. Irmak [12] presented DCNN with a fully optimized model for multi-classification of MRI brain tumor images. The developed model significantly classifies the brain tumors into three grades (Grade IV, III, and II), and five types (metastatic, pituitary, meningioma, glioma, and normal). The implemented model obtained satisfactory classification results on the publicly and larger clinical databases, where the obtained results were superior compared to the existing deep learning models. The DCNN with a fully optimized model assists radiologists and physicians in initial screening of brain tumors, but it was computationally expensive. Further, S. Deepak and P.M. Ameer, [13] adopted deep-transfer learning concept with a GoogleNet pre-trained model for BTC by using MRI brain tumor images. As denoted in the resulting section, the developed model's efficacy was investigated by means of specificity, F1-score, recall, area under the curve and precision, however, the phenomenon of over-fitting was observed in the developed model.

J.D. Bodapati, et al, [14] extracted local features from the convolution blocks of Xception and Inception-ResNet V2 networks. The extracted features were vectorised by using pooling-based methods. Additionally, an attention process was performed to classify the sub-types of tumor present in the MRI brain images. However, the presented model needs a larger amount of data to achieve high classification results where it was computationally expensive. Further, S. Kokkalla, et al, [15] has introduced a new

deep dense inception residual network for BTC. As stated in the resulting segment, the presented model has obtained only comparable results on the noisy MRI brain images. In addition, the developed model still needs to be focused on the computational time and reduction of the number of parameters. Alhassan and Zainon [16] utilized image normalization approach and Histogram of Oriented Gradient (HOG) [26] descriptor for denoising and feature extraction. Additionally, the extracted features were fed to the CNN model with the Hard Swish based Rectified Linear Unit (ReLU) activation function for BTC. The conducted experiment demonstrated that the implemented model has achieved significant classification accuracy but the computational time was higher while training the model on the larger unstructured databases.

V.V.S. Sasank and S. Venkateswarlu, [17] integrated contrast limited adaptive histogram equalization technique and Laplacian of Gaussian approach for image denoising. Further, the tumor region was segmented by implementing fuzzy c means, and then, the feature extraction was carried-out utilizing three global-level-descriptors. The extracted features were optimally reduced and classified by the kernel based soft-plus extreme learning machine technique, but the developed model was computationally complex. A. Dixit and A. Nanda [18] integrated an improved whale optimizer with a radial basis neural network for effective BTCs. As stated in the resulting section, the developed model has obtained higher classification accuracy, but the network size was larger, which was computationally expensive. C.S. Rao and K. Karunakara, [19] initially performed image denoising utilizing normalized median filter and blur-removal. Further, the Spatial Grey-level Dependence Matrix (SGLDM) and Gray-level Co-occurrence Matrix (GLCM) were utilized to extract relevant features which were further fed to the Harris Hawks Optimizer (HHO) for feature selection. Next, a Kernel based Support Vector Machine (K-SVM) was used to classify the sub-types of brain tumor. The developed K-SVM classifier supports only binary classification, which was in-appropriate in multiclass classification. S.K. Mohapatra et al, [20] has used fuzzy c means, Particle Swarm Optimizer (PSO), and Extreme Learning Machine (ELM) for brain tumor segmentation and tumor subtype classification. The presented ELM model was computationally complex, so, a modified CNN is implemented in this manuscript to overcome the afore-mentioned issues and to achieve better BTC.

Hafiz Aamir Hafeez, et al, [32] have been developed CNNs and employed for the purpose of classifying glioma grading, specifically distinguishing between low grade (grade I-II) and high grade (grade III-IV). A lightweight CNN-based model has been suggested, characterized by its reduced number of layers, smaller size, and fewer learnable parameters. The researchers conducted experimental trials on well-established publicly accessible datasets, such as Brats-2017, Brats-2018, and Brats-2019. The outputs of the experiments and research have been cross-validated using a dataset obtained from Bahawal Victoria Hospital, located in Bahawalpur, Pakistan. The model under consideration demonstrated optimal performance on the standardized evaluation metrics for the dataset in question, specifically accuracy, specificity, and sensitivity. An additional improvement in this study would involve categorizing glioma grades into four distinct types, namely grade I to grade IV. Furthermore, it would be beneficial to classify glioma types into specific categories such as astrocytomas, oligodendrogliomas, and brainstem gliomas, among others.

### 3. Methodology

The automated segmentation and categorization of medical pictures have been increasingly important in the prediction of growth, diagnosis, and therapy of brain tumors in recent times. Early detection of brain tumors is associated with improved treatment outcomes, leading to enhanced patient survival rates. The proposed study includes three major phases like image acquisition: BRATS 2018, 2019, and 2020 databases, image denoising: Gaussian blur[25] and contour approximation techniques, and tumor classification: Modified CNN model. The block diagram of the proposed study is denoted in figure 1.

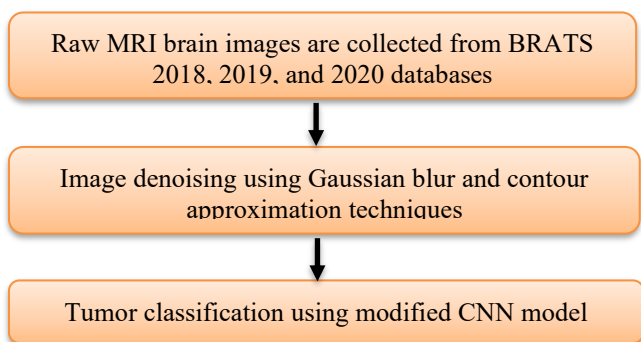


Fig. 1. Block diagram of the proposed study

#### 3.1. Image Acquisition

The proposed modified CNN model's efficacy is tested on three online databases such as BRATS 2018, 2019, and 2020 databases. The BRATS 2018 database consists of 210 and 75 higher and lower grade gliomas brain images [21]. In addition, the BRATS 2019 database consists of 259 and 76 higher and lower grade gliomas brain images with the pixel resolution size of  $240 \times 240 \times 155$  [22]. Further, the BRATS 2020 database consists of 369 individuals higher and lower grade gliomas brain images, which are categorized into four modalities such as T2-fluid attenuated inversion recovery, T1-native, T2-weighted, and Post Contrast T1-CE [23][29]. The acquired sample MRI brain images are represented in figure 2.

Database available links:

**BRATS 2018:** <https://paperswithcode.com/dataset/brats-2018-1>

**BRATS 2019:** [https://github.com/woodywff/brats\\_2019](https://github.com/woodywff/brats_2019)

**BRATS 2020:** <https://www.kaggle.com/awsaf49/brats2020-training-data>

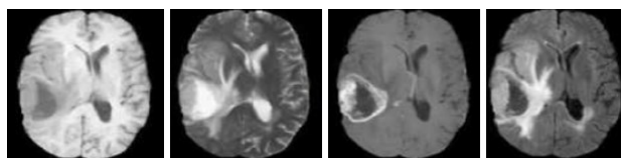


Fig. 2. Images showing the eviusual symptoms cause by fungal disease

#### 3.2. Image Denoising

The acquired sample MRI brain images are denoised by employing Gaussian blur and contour approximation technique. Firstly, the Gaussian blurring technique applied a low-pass filter in the acquired MRI brain images for removing Gaussian noise. The

Gaussian blur is an image blurring filter, which utilizes a Gaussian function for computing the transformations of every pixel in the MRI brain images. The mathematical equation of Gaussian blur is specified in equation (1). On the other hand, the contour approximation utilizes rammer-douglas-peucker methodology for simplifying the image polyline which decreases the vertices for better image representation [24].

$$G(u, v) = \frac{1}{2\pi\sigma^2} e^{-\frac{u^2+v^2}{2\sigma^2}} \quad (1)$$

Where,  $\sigma$  indicates standard deviations of the gaussian distributions,  $u$  and  $v$  are the distance from the original in the vertical and horizontal axis. The denoised sample MRI brain images are depicted in figure 3.

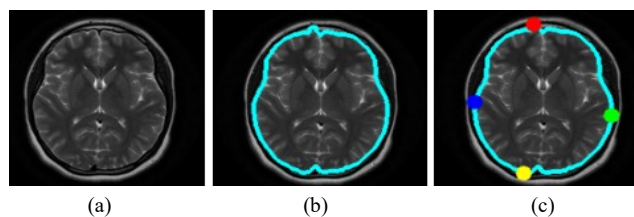


Fig. 3. a) Output of Gaussian blur, b) output of contour approximation, and c) extreme points

#### 3.3. Tumor classification

After identifying RoI from the denoised images, the tumor classification is performed by using a modified CNN model. In recent periods, the CNN models exhibited great potential in brain tumor segmentation [28][30] and classification, because the deep learning models are superior in learning the local and global structure of the MRI brain images. In this research article, the ReduceLRonPlateau function is added with the CNN model for brain lesion segmentation and subtypes of tumor classification. In the modified CNN model, the convolutional layers are the primary layers, where two dimensional metrics  $T_i$  are given as the input to the convolutional layers  $l$ . The convolutional layers have a set of filters where every filter is convolved with the metrics  $T_i$  in order to compute the activation maps. By stacking the activation maps of all the filters, the output of the convolutional layer is achieved. Hence, the mapping operations in the convolutional layers are mathematically determined in equation (2).

$$T_j^l = f(x) \left( \sum_{i \in M_j} T_i^{l-1} \times k_{i,j}^l + \theta_j^l \right) \quad (2)$$

Where,  $f(x)$  specifies ReLU activation functions,  $T_i^{l-1}$  represents  $i^{th}$  feature sub-sets of  $(l-1)$  convolutional layers,  $\theta_j^l$  denotes bias,  $T_j^l$  states  $j^{th}$  mapping set of the convolutional layers, and  $k_{i,j}^l$  represents convolutional kernels between  $i^{th}$  feature sub-sets and  $j^{th}$  mapping set in the convolutional layers. The max-pooling process is the next step in the modified CNN that decreases the overfitting concern during data training.

The max-pooling operation is a vital step in the modified CNN model for feature extraction and dimensionality reduction. This operation is performed for integrating the neighbourhood elements in the convolutional output metrics to decrease output neurons in the convolutional layers. In this manuscript, the max-pooling layers have a kernel size of  $3 \times 3$  for selecting the maximum

values from 4 neighbourhood elements to generate one output matrix element. The max-pooling layer is represented in equation (3).

$$T_j^l = f(x)(\beta_j^l \text{down}(T_i^{l-1}) + \theta_j^l) \quad (3)$$

Where,  $\text{down}(T_i^{l-1})$  states down sampling from  $(l-1)$  layer to  $l^{\text{th}}$  layer,  $\theta_j^l$  denotes additive bias,  $\beta_j^l$  represents multiplicative bias, and  $f(x)$  indicates ReLU activation function. Further, the matrix feature values of the max-pooling layers are arranged for generating a rasterization layer, which is connected with the fully connected layers  $h_j$ . Though, the output of the fully-connected layers are depicted in equation (4).

$$h_j = f(x)(\sum_{i=0}^{n-1} w_{i,j} T_i - \theta_j) \quad (4)$$

Where,  $w_{i,j}$  indicates the weight connection of input vectors  $T_i$  and  $\theta_j$  denotes node threshold value. In the modified CNN, the soft-max layers are applied as the fully-connected layers for dealing the multi-class classification problems. In the soft-max layers, the cross entropy loss-function is utilized for controlling the network output, and it is mathematically represented in equation (5).

$$J(\theta) = -\frac{1}{M} [\sum_{i=1}^M \sum_{j=1}^k l\{y^{(i)} = j\} \log \frac{e^{\theta_j^i}}{\sum_k e^{\theta_k^i}}] \quad (5)$$

Where,  $l(\cdot)$  represents indicator function,  $\frac{e^{\theta_j^i}}{\sum_k e^{\theta_k^i}}$  indicates output of  $j^{\text{th}}$  neurons,  $e$  denotes the constant value,  $\sum_k e^{\theta_k^i}$  represents input of all neurons, and  $e^{\theta_j^i}$  indicates input of  $j^{\text{th}}$  neurons. At last, the rule items and ReduceLRonPlateau function are incorporated with  $J(\theta)$  to prevent data falling into local optima and for early stopping criteria. The updated cross-entropy loss-function in the soft-max layers is mentioned in equation (6).

$$J(\theta) = -\frac{1}{m} \left[ \sum_{i=1}^m \sum_{j=1}^k l\{y^{(i)} = j\} \log \frac{e^{\theta_j^i}}{\sum_k e^{\theta_k^i}} \right] + \frac{\rho}{2} \sum_{i=1}^k \sum_{j=0}^n \theta_{ij}^2 \quad (6)$$

Where,  $\frac{\rho}{2} \sum_{i=1}^k \sum_{j=0}^n \theta_{ij}^2$  indicates a weight function, which is utilized to stabilize the excessive parameters in both testing and training set. The hyper-parameter setting of the modified CNN model is denoted as follows: loss: cross entropy loss function, optimizer: ADAM, activation function: ReLU, number of hidden layers: 10, and number of epochs: 100. The experimental results of the modified CNN model are represented in the upcoming section, and the output of the modified CNN model is depicted in figure 4.

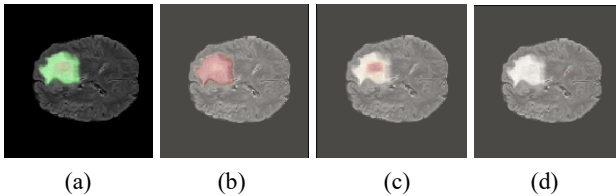


**Fig. 4.** Segmented image of modified CNN model: a) all classes, b) WT, c) TC, and d) ET

## 4. Simulation results

Anaconda Navigator 3.5.2.0 (64-bit) was used to implement and test the new CNN model in Python 3.9. The improved Convolutional Neural Network (CNN) model is tested on a

machine with 128GB of random-access memory, an Intel Core i9 CPU, a 22GB-RTX-2080-Ti graphics processing unit, and Windows 10 (64-bit). The experimental assessment uses Sea-born, Matplotlib, Keras, Open-CV, time, Math, Sklearn, TQDM, and TensorFlow Python libraries. The improved CNN model for the BRATS 2018, 2019, and 2020 databases is evaluated using accuracy, specificity, NPV, sensitivity, and PPV. As three different case studies, the efficiency of the results derived in each of these case studies are also subjected with respect to the proposed metrics. The evaluation is carried out in the same environment for each of the models and the predicted outcomes are also presented in its right perspective. BTC accuracy is the ratio of accurate forecasts to total predictions. The accuracy of total positive and negative outcomes is measured by sensitivity and specificity. Positive Predictive Value (PPV) is derived by dividing True Positives (TPs) by positive cases. Negative Predictive Value (NPV) is calculated by dividing True Negatives (TNs) by negative instances. Accuracy, specificity, NPV, sensitivity, and PPV are represented mathematically in Equations (7-11). TN, FN, FP, and TP stand for true negative, false negative, false positive, and true positive. An example confusion matrix is shown in Figure 5.

$$\text{Accuracy} = \frac{TP+TN}{TP+TN+FP+FN} \times 100 \quad (7)$$

$$\text{Specificity} = \frac{TN}{TN+FP} \times 100 \quad (8)$$

$$\text{NPV} = \frac{TN}{TN+FN} \times 100 \quad (9)$$

$$\text{Sensitivity} = \frac{TP}{TP+FN} \times 100 \quad (10)$$

$$\text{PPV} = \frac{TP}{TP+FP} \times 100 \quad (11)$$

On the other hand, the segmentation performance of the developed modified CNN model is evaluated by utilizing the evaluation metrics such as JC and DSC values. The JC and DSC are spatial overlap indexes, which determine the percentage of overlap between the predicted output image and target mask. The mathematical representations of JC and DSC are depicted in equations (12) and (13).

$$\text{DSC} = \frac{2TP}{2TP+FN+FP} \times 100 \quad (12)$$

$$\text{JC} = \frac{FP+FN}{TP+TN+FP+FN} \times 100 \quad (13)$$

### 4.1. Quantitative investigation

In this scenario, the segmentation results of the modified CNN model and the comparative models: k-means and CNN are denoted in table 1. As stated in table 1, the proposed modified CNN model has achieved high segmentation results by means of JC and DSC, and the results are individually validated on three tumor sub-regions like Enhancing-Tumors (ETs), Tumor-Cores (TCs), and Whole-Tumors (WTs) regions. By investigating table 1, the modified CNN model has obtained a mean DSC value of 94.23%, 93.55%, and 92.01% on the BRATS 2018, 2019 and 2020 databases. Additionally, the modified CNN model achieved a

mean JC value of 89.73%, 90.04% and 85.43% on the BRATS 2018, 2019 and 2020 databases. The efficacy of the model is subjected to the process of segmentation by converting the unstructured data into structured data and further classification is carried out. The models used for segmentation and classification are also presented. The segmentation results obtained are highly



Fig. 5. Sample confusion matrix

Table 1. Segmentation results of the modified CNN model and the comparative models

Models	Database	WT		TC		ET	
		DSC(%)	JC(%)	DSC(%)	JC(%)	DSC(%)	JC(%)
K-means	BRATS 2018	90.91	88.52	83.29	81.28	84.74	80.84
CNN		94.38	90.53	90.83	83.47	88.40	78.66
<b>Modified CNN</b>		<b>98.90</b>	<b>95.60</b>	<b>93.07</b>	<b>88.82</b>	<b>90.72</b>	<b>84.78</b>
K-means	BRATS 2019	90.82	92.04	89.89	88.40	78.63	77.40
CNN		93.49	94.35	88.65	90.63	80.46	79.75
<b>Modified CNN</b>		<b>96.22</b>	<b>95.45</b>	<b>94.55</b>	<b>91.98</b>	<b>89.89</b>	<b>82.70</b>
K-means	BRATS 2020	94.20	91.02	82.38	73.20	82.02	72.03
CNN		95.32	93.20	88.48	75.04	84.50	75.55
<b>Modified CNN</b>		<b>97.24</b>	<b>94.63</b>	<b>90.06</b>	<b>81.93</b>	<b>88.73</b>	<b>79.75</b>

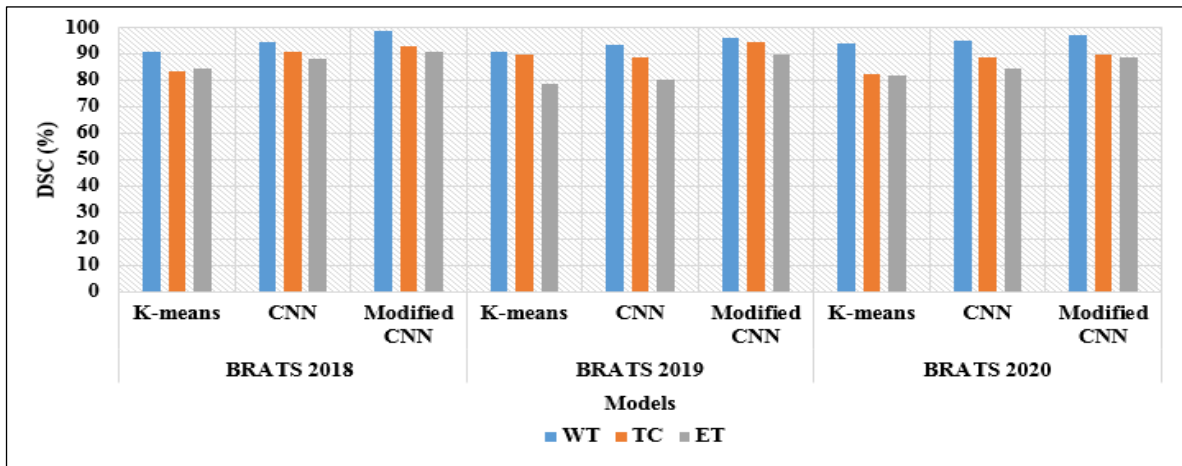


Fig 6. Graphical analysis of the modified CNN model and the comparative models by means of DSC value

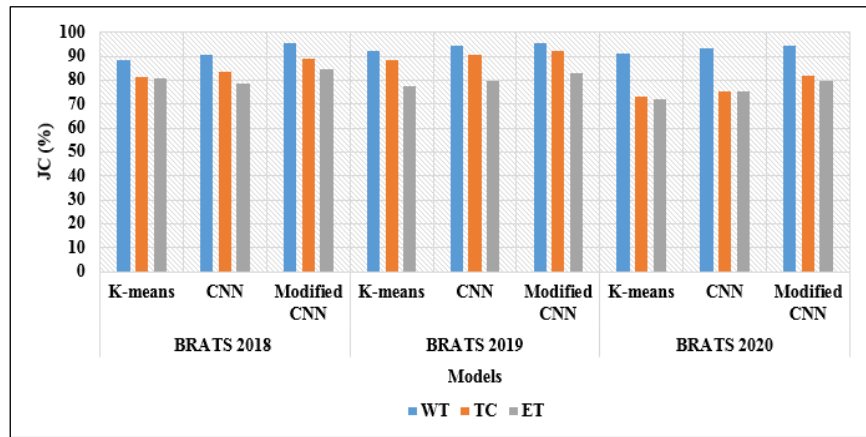


Fig 7. Graphical analysis of the modified CNN model and the comparative models in light of JC value

Table 2. Classification results of the modified CNN model and the comparative models

Models	Database	Accuracy (%)	Specificity (%)	NPV (%)	Sensitivity (%)	PPV (%)
SVM	BRATS 2018	93.82	92.93	94.37	93.20	92.10
KNN		95.55	96.03	95.34	96.30	94.39
CNN		98.93	98.72	95.94	96.48	95.22
<b>Modified CNN</b>		<b>99.87</b>	<b>100</b>	<b>98.58</b>	<b>100</b>	<b>99.23</b>
SVM	BRATS 2019	96.76	95.20	94.30	93.30	92.75
KNN		95.40	97.05	95.05	96.98	94.76
CNN		97.87	94.21	95.90	94.78	98.27
<b>Modified CNN</b>		<b>99.80</b>	<b>100</b>	<b>98.32</b>	<b>100</b>	<b>99.40</b>
SVM	BRATS 2020	96.92	92.20	92.01	91.02	94.39
KNN		97.10	94.39	93.26	93.20	95.02
CNN		97.70	95.32	94.28	95.74	97.20
<b>Modified CNN</b>		<b>99.63</b>	<b>100</b>	<b>97.12</b>	<b>100</b>	<b>98.84</b>

correlated with existing models such as K-means and CNN. Figures 6 and 7 depict the graphical analysis of the improved M-CNN model and the comparable models, using the DSC and JC.

Additionally, the classification results of the modified CNN model and the comparative models are specified in table 2. By investigating table 2, the developed modified CNN model achieved maximum classification results compared to other existing models like SVM, CNN, and K-Nearest Neighbor (KNN) in terms of accuracy, specificity, NPV, sensitivity, and PPV. As specified in table 2, the modified CNN model achieved 99.87%, 99.80%, and 99.63% of accuracy, 100% of specificity and sensitivity on the BRATS 2018, 2019, and 2020 databases. Additionally, the modified CNN model has obtained 98.58%, 98.32%, and 97.12% of NPV, and 99.23%, 99.40%, and 98.84% of PPV on the BRATS 2018, 2019, and 2020 databases. In addition, the achieved experimental results are high related to other classification techniques. Graphical representation of the modified CNN model in terms of accuracy, specificity, NPV, sensitivity and PPV is stated in figure 8.

BRATS 2018, 2019, and 2020 databases, which are significantly minimum related to the existing models. Further, the system complexity is linear, which is computed on the basis of order of magnitude and input data size.

#### 4.2. Comparative investigation

In this section, the proposed modified CNN model's efficiency is validated by comparing its performance with the existing studies, and the results are stated in table 3. C.S. Rao and K. Karunakara [19] used normalized median filtering technique for blur removal and further, the feature extraction was performed by employing SGLDM and GLCM descriptors. In addition, the extracted features were dimensionally diminished utilizing HHO technique, and lastly, the sub-types of the brain tumors were classified by implementing K-SVM classifier. Simulation results demonstrated that the developed model has obtained 99.20%, 99.36%, and 99.15% of classification accuracy on the BRATS 2018, 2019, and 2020. Additionally, S.K. Mohapatra et al, [20] integrated fuzzy C means, PSO, and ELM for effective brain tumor

segmentation and sub-type classification of the brain tumors. The extensive experimental investigations showed that the presented model has attained 99.47% of classification accuracy on the BRATS 2020. Related to these comparative studies, the developed modified CNN model attained maximum classification accuracy of 99.87%, 99.80% and 99.63% on the BRATS 2018, 2019, and 2020. The inclusion of the ReduceLRonPlateau function in the CNN model helps in decreasing the system complexity and computational time, which are the major problems highlighted in the related work section.

The works contributed by the authors Ujjwal Baid, Satyam Ghodasara, et al., (2021) [31], Yun Jiang, Yuan Zhang, et al., (2022) [32], Linmin pie and Yanling Liu, (2022) , Ramy A. Zeineldin, et al., (2022) are also considered to rate the efficiency of the developed model. From the outputs it is clearly observed that our model outperforms in terms of accuracy with respect to BRATS dataset ranging from 2018 to 2022.

**Table 3.** Comparative results of the modified CNN model and the existing studies

Models	Database	Accuracy (%)
HHO-K-SVM [19]	BRATS 2018	99.20
	BRATS 2019	99.36
	BRATS 2020	99.15
PSO-ELM [20]	BRATS 2020	99.47
<b>Modified CNN</b>	<b>BRATS 2018</b>	<b>99.87</b>
	<b>BRATS 2019</b>	<b>99.80</b>
	<b>BRATS 2020</b>	<b>99.63</b>

approximation techniques. The under-taken techniques effectively eliminates the Gaussian noise from the acquired raw MRI brain images, and further, provides a better image representation. The denoised images are given to the modified CNN model for brain lesion segmentation and sub-types of tumor classification such as WT, TC, and ET. The modified CNN model comprises ReduceLRonPlateau function for early stopping criteria that significantly decreases the system complexity and computational time. On the other hand, the evaluation metrics like accuracy, specificity, NPV, sensitivity, PPV, JC, and DSC are utilized to validate the segmentation and classification performance of the modified CNN model. The simulation outcome indicate that the modified CNN model achieved better BTC performance compared to the existing models: HHO-KSVM and PSO-ELM. As indicated in the resulting section, the modified CNN model has achieved 99.87%, 99.80%, and 99.63% of accuracy on the BRATS 2018, 2019 and 2020 databases with a classification loss of 0.0198. As the future extension, a novel ensemble based deep learning method and hybrid clustering technique can be included to further improve brain lesion segmentation and tumor sub-type classification.

### Author contributions

**G V Sivanarayana:** Image Analysis, Machine Learning and Deep Learning

**Dr. K Naveen Kumar:** Image Analysis, Internet of Things, & Network Security

### Funding:

The authors have no affiliation with any organization with a direct or indirect financial interest in the subject matter discussed in the manuscript. No funding was received for conducting this study

### Conflict of Interest:

All authors have participated in analysis and interpretation of the data, drafting the article for important intellectual content. This manuscript has not been submitted to, nor is under review at, another journal or other publishing venue.

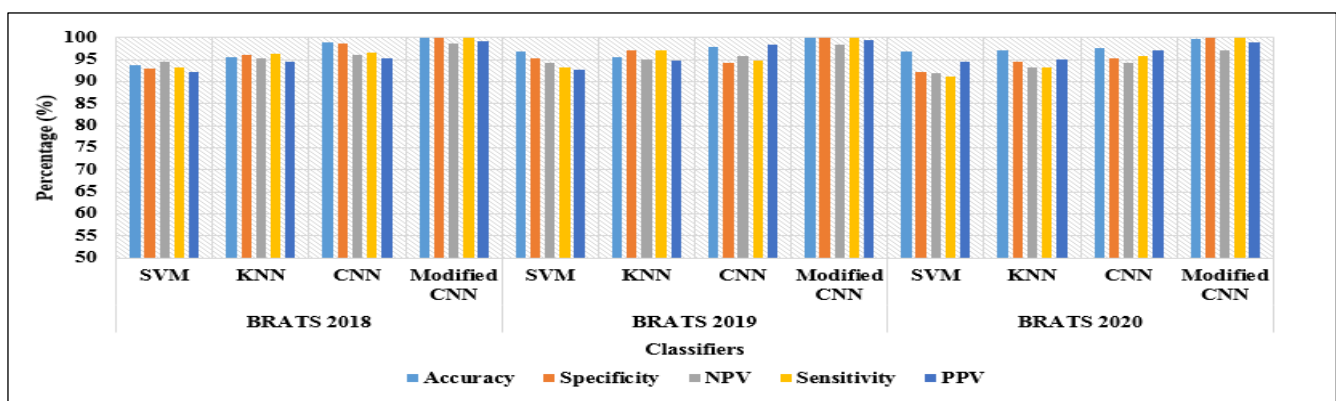


**Fig 8.** Graphical analysis of the modified CNN model and the comparative models in light of accuracy, specificity, NPV, sensitivity, and PPV

### 5. Conclusion

In this research manuscript, a modified CNN model is implemented for effective BTC, whereas the proposed study majorly includes three phases. After acquiring the raw MRI brain images from BRATS 2018, 2019 and 2020 databases, the image denoising is performed using Gaussian blur and contour

### References

- [1] F.J. Díaz-Pernas, M. Martínez-Zarzuela, M. Antón-Rodríguez, and D. González-Ortega, "A deep learning approach for brain tumor classification and segmentation using a multiscale convolutional neural network", In Healthcare, Multidisciplinary Digital Publishing Institute, vol.9, no.2, pp.153, 2021..
- [2] J. Kang, Z. Ullah, and J. Gwak, "MRI-based brain tumor

- classification using ensemble of deep features and machine learning classifiers”, *Sensors*, vol.21, no.6, pp.2222, 2021.
- [3] M.I. Sharif, M.A. Khan, M. Alhussein, K. Aurangzeb, and M. Raza, “A decision support system for multimodal brain tumor classification using deep learning”, *Complex & Intelligent Systems*, pp.1-14, 2021.
- [4] R. Singh, A. Goel, and D.K. Raghuvanshi, “Computer-aided diagnostic network for brain tumor classification employing modulated Gabor filter banks”, *The Visual Computer*, vol.37, no.8, pp.2157-2171, 2021.
- [5] T. Sadad, A. Rehman, A. Munir, T. Saba, U. Tariq, N. Ayesha, and R. Abbasi, “Brain tumor detection and multi-classification using advanced deep learning techniques”, *Microscopy Research and Technique*, vol.84, no.6, pp.1296-1308, 2021.
- [6] F. Bashir-Gonbadi, and H. Khotanlou, “Brain tumor classification using deep convolutional autoencoder-based neural network: Multi-task approach”, *Multimedia Tools and Applications*, vol.80, no.13, pp.19909-19929, 2021.
- [7] N. Kesav, and M.G. Jibukumar, “Efficient and low complex architecture for detection and classification of Brain Tumor using RCNN with Two Channel CNN”, *Journal of King Saud University-Computer and Information Sciences*, 2021.
- [8] A.R. Khan, S. Khan, M. Harouni, R. Abbasi, S. Iqbal, and Z. Mehmood, “Brain tumor segmentation using K-means clustering and deep learning with synthetic data augmentation for classification”, *Microscopy Research and Technique*, vol.84, no.7, pp.1389-1399, 2021.
- [9] S. Krishnakumar, and K. Manivannan, “Effective segmentation and classification of brain tumor using rough K means algorithm and multi kernel SVM in MR images”, *Journal of Ambient Intelligence and Humanized Computing*, vol.12, no.6, pp.6751-6760, 2021.
- [10] S. Deepak, and P.M. Ameer, “Automated categorization of brain tumor from MRI using CNN features and SVM”, *Journal of Ambient Intelligence and Humanized Computing*, vol.12, no.8, pp.8357-8369, 2021.
- [11] W. Ayadi, W. Elhamzi, I. Charfi, and M. Atri, “Deep CNN for brain tumor classification”, *Neural Processing Letters*, vol.53, no.1, pp.671-700, 2021.
- [12] E. Irmak, “Multi-classification of brain tumor MRI images using deep convolutional neural network with fully optimized framework”, *Iranian Journal of Science and Technology, Transactions of Electrical Engineering*, vol.45, no.3, pp.1015-1036, 2021.
- [13] S. Deepak, and P.M. Ameer, “Brain tumor classification using deep CNN features via transfer learning”, *Computers in biology and medicine*, vol.111, pp.103345, 2019.
- [14] J.D. Bodapati, N.S. Shaik, V. Naralasetti, and N.B. Mundukur, “Joint training of two-channel deep neural network for brain tumor classification”, *Signal, Image and Video Processing*, vol.15, no.4, pp.753-760, 2021.
- [15] S. Kokkalla, J. Kakarla, I.B. Venkateswarlu, and M. Singh, “Three-class brain tumor classification using deep dense inception residual network”, *Soft Computing*, vol.25, no.13, pp.8721-8729, 2021.
- [16] A.M. Alhassan, and W.M.N.W. Zainon, “Brain tumor classification in magnetic resonance image using hard swish-based RELU activation function-convolutional neural network”, *Neural Computing and Applications*, vol.33, no.15, pp.9075-9087, 2021.
- [17] V.V.S. Sasank, and S. Venkateswarlu, “Brain tumor classification using modified kernel based softplus extreme learning machine”, *Multimedia Tools and Applications*, vol.80, no.9, pp.13513-13534, 2021.
- [18] A. Dixit, and A. Nanda, “An improved whale optimization algorithm-based radial neural network for multi-grade brain tumor classification”, *The Visual Computer*, pp.1-16, 2021.
- [19] C.S. Rao, and K. Karunakara, “Efficient detection and classification of brain tumor using kernel based SVM for MRI”, *Multimedia Tools and Applications*, vol.81, no.5, pp.7393-7417, 2022.
- [20] S.K. Mohapatra, P. Sahu, J. Almotiri, R. Alroobaea, S. Rubaiee, A. Bin Mahfouz, and A.P. Senthilkumar, “Segmentation and Classification of Encephalon Tumor by Applying Improved Fast and Robust FCM Algorithm with PSO-Based ELM Technique”, *Computational Intelligence and Neuroscience*, 2022.
- [21] A. Rehman, M.A. Khan, T. Saba, Z. Mehmood, U. Tariq, and N. Ayesha, “Microscopic brain tumor detection and classification using 3D CNN and feature selection architecture”, *Microscopy Research and Technique*, vol.84, no.1, pp.133-149, 2021.
- [22] M.I. Sharif, J.P. Li, J. Amin, and A. Sharif, “An improved framework for brain tumor analysis using MRI based on YOLOv2 and convolutional neural network”, *Complex & Intelligent Systems*, vol.7, no.4, pp.2023-2036, 2021.
- [23] M. Lin, S. Momin, Y. Lei, H. Wang, W.J. Curran, T. Liu, and X. Yang, “Fully automated segmentation of brain tumor from multiparametric MRI using 3D context deep supervised U-Net”, *Medical Physics*, vol.48, no.8, pp.4365-4374, 2021.
- [24] Y.Q. Liu, X. Du, H.L. Shen, and S.J. Chen, “Estimating generalized Gaussian blur kernels for out-of-focus image deblurring”, *IEEE Transactions on circuits and systems for video technology*, vol.31, no.3, pp.829-843, 2020.
- [25] Ravindra K. Purwar & Varun Srivastava, “A novel feature based indexing algorithm for brain tumor MR-images”, *International Journal of Information Technology*, vol.12, pp.1005-1011, 2020.
- [26] Tanmoy Kanti Halder, Kanishka Sarkar, Ardhendu Mandal and Suvro Sarkar, “A novel histogram feature for brain tumor detection”, *International Journal of Information Technology*, vol.14, pp. 1883-1892, 2022.
- [27] Singh, R., Agarwal, B.B, “An automated brain tumor classification in MR images using an enhanced convolutional neural network”, *International Journal of Information Technology*, volume 15, pp. 665-674, 2023.
- [28] Ujjwal Baid, Satyam Ghodasara, et al., “The RSNA-ASNR-MICCAI BraTS 202 Benchmark on Brain Tumor Segmentation and Radiogenomic Classification”, arXiv:2107.02314v2 [cs.CV] 12 Sep 2021.
- [29] Yun Jiang, Yuan Zhang, et al., “SwinBTS: A Method for 3D Multimodal Brain Tumor Segmentation Using Swin Transformer”, *Brain Sciences*, MDPI, volume 12, pp. 797, 2022. <https://doi.org/10.3390/brainsci12060797>
- [30] Linmin Pie, Yanling Liu, “Multimodal Brain Tumor Segmentation using a 3D ResUNet in BraTS 2021”, *BrainLes 2021. Lecture Notes in Computer Science*, Springer, volume 12962, 2022. [https://doi.org/10.1007/978-3-031-08999-2\\_26](https://doi.org/10.1007/978-3-031-08999-2_26).
- [31] Ramy A. Zeineldin, et al., “Multimodal CNN Networks for Brain Tumor Segmentation in MRI: A BraTS 2022 Challenge Solution”, arXiv:2212.09310, 2022, <https://doi.org/10.48550/arXiv.2212.09310>.
- [32] H. A. Hafeez et al., "A CNN-Model to Classify Low-Grade and High-Grade Glioma From MRI Images", *IEEE Access*, vol. 11, 2023, pp. 46283-46296, doi: 10.1109/ACCESS.2023.3273487.